Journal Name

Dynamic Article Links ►

Cite this: DOI: 10.1039/c0xx00000x

www.rsc.org/xxxxxx

ARTICLE TYPE

Investigation of a copper(I) biquinoline complex for application in dye-sensitized solar cells

Kathryn A. Wills[a], Humberto J. Mandujano-Ramírez[b], Gabriel Merino[b], Davide Mattia[a], Gerko Oskam[b], Matthew D. Jones[a], Simon E. Lewis[a] and Petra J. Cameron[a]*

Received (in XXX, XXX) Xth XXXXXXXXX 20XX, Accepted Xth XXXXXXXXX 20XX
DOI: 10.1039/b000000x

The synthesis, properties and application of a [Cu(2,2'-biquinoline-4,4'-dicarboxylic acid)$_2$] complex in dye-sensitized solar cells (DSSC) is described. The complex is electrochemically stable and strongly absorbing with a molar extinction coefficient at $\lambda_{(max)}$ 564 nm of 11,700 $M^{-1}cm^{-1}$ (in MeOH). Experimental and computational data indicate the HOMO, LUMO and electronic excited state energy levels are appropriate for functionality in a DSSC. From cyclic voltammetry the HOMO is estimated to be -5.27 eV, which is supported by computational work, which locates the HOMO at -5.78 eV. From electrochemical, absorption and emission experiments, the MLCT energy levels are expected to be appropriate for electron injection into the TiO_2 conduction band. Our computations support this and locate the key MLCT at 563 nm. Despite this the efficiency in DSSC is extremely low (<0.1%) suggesting that the dye does not inject excited electrons into the TiO_2 conduction band.

Over the past two decades, dye-sensitized solar cells (DSSCs) have established themselves as a promising and versatile technology for converting solar energy into electrical energy.[1, 2] Improving the performance of the photosensitizing component in DSSCs has been extensively investigated, however the most stable are still generally ruthenium(II) complexes.[3] Interest has grown in the replacement of ruthenium with a less expensive and more abundant metal, such as copper, to create complexes which have similar properties for DSSC application but without relying on a scarce resource.[4, 5]

Copper(I) dyes have not yet been as extensively studied as their ruthenium(II) counterparts, although some very promising experimental and computational studies have been published in recent years.[6-17] The most efficient Cu(I) dyes to date have been developed by Constable and co-workers who have obtained solar conversion efficiencies of ≥2% with both homoleptic[7] and, more recently, heteroleptic[8, 9, 17] complexes. An *in situ* ligand exchange strategy has enabled the group to screen a large range of ligand combinations in DSSCs. These Cu(I) complexes consist of one anchoring ligand and a second, non-anchoring, ligand. Functionalisation of a non-anchoring 2,2'-bipyridine ligand with a heteroaromatic[9] or a bulky diphenylamino[8] substituent have produced impressive DSSC performances attributed, in part, to an extended π-system relative to the simple bipyridyl ligand. The group's highest DSSC efficiency so far is 3.77%, which employed a phosphonate anchoring ligand and a 2,2-bipyridine ligand bearing hole-transporting triphenylamino substituents.[17] There have also been reports of copper(I) DSSC which replace the conventional I^-/I_3 electrolyte with $[Co(L)_3]^{2+/3+}$ mediators, where L is either 2,2-bipyridine or 1,10- phenanthroline.[14, 15] In addition, a recent theoretical investigation by Lu *et al*., has noted the benefits of modifying the traditional bipyridyl ligand structure by extending the conjugation of the system.[11] In order to create a dye with improved spectral coverage, we are investigating ligands which are commercially available or else straightforward to synthesise. Since we aim to devise more sustainable dyes using an abundant metal, it is important that our choice of ligand corresponds as far as possible with this objective.

Whilst organic dyes are often quoted as being a sustainable alternative to ruthenium based dyes, their disadvantages are frequently overlooked. Organic dyes do generally have higher molar extinction coefficients than metal complexes, but their absorption bands in the visible region are generally narrower[18] (typically $\Delta\lambda$ ~ 100-250 nm compared to $\Delta\lambda$ ~ 350 nm in the broader absorption bands of metal complexes).[19] It is also noted that organic dyes can suffer from increased recombination reactions, compared to the ruthenium complex N719, when I^-/I_3^- is used as the redox species.[20] Finally, in order to obtain the highest efficiencies, organic dyes (and porphyrins and phthalocyanines) need to be very carefully designed on a molecular level, which usually necessitates multi-step syntheses.[21-23] To exemplify, DSSC with > 12% efficiency have been prepared using a mixture of a porphyrin dye and the organic dye Y123.[23] The porphyrin dye is the product of an 8 step synthesis and Y123 requires a 9 step synthesis.[22] Purification of

[a] *Doctoral Training Centre in Sustainable Chemical Technologies, University of Bath, Bath, BA2 7AY, UK. Fax: +44(0)1225 386231; Tel: +44 (0)1225 386116. E-mail: p.j.cameron@bath.ac.uk.*
[b] CINVESTAV IPN, Dept Fis Aplicada, Merida 97310, Yucatan, Mexico† Electronic Supplementary Information (ESI) available: [details of any supplementary information available should be included here]. See DOI: 10.1039/b000000x/

these dyes is also non-trivial.

The copper (I) biquinoline complex described here is not the result of a long synthetic pathway and the suitability of copper (I) complexes generally in DSSCs is noted in the literature.[4, 11, 24] To that end, we have synthesised and assessed the properties of a copper(I) dye with the commercially available 2,2'-biquinoline-4,4'-dicarboxylic acid (dcbiq) ligand (or bicinchoninic acid, BCA). $[Cu(dcbiq)_2]^+$ is a known compound and is most commonly used in the BCA assay, which measures protein concentration in a solution.[25, 26] Odobel and co-workers recently reported the synthesis of heteroleptic copper(I) complexes which employed an anchoring ($dcbiqH_2$) ligand and sterically bulky variants of the 1,10-phenanthroline ligand.[13] The route to synthesis of these dyes chooses a chelating ligand which is so bulky as to make formation of the homoleptic species highly unfavourable. Some similarities between these species and the title complex in this paper will be noted later. Analogous ruthenium(II) biquinoline complexes, both heteroleptic[27, 28] and homoleptic[29] have been trialled, although their DSSC properties and performance were poorer than for other ruthenium sensitizers. Incident photon-to-current efficiencies (IPCEs) for the heteroleptic ruthenium complexes were low (≤ 10%). Homoleptic sensitizers of the type *cis*-$Ru(dcbiq)_2(NCS)_2$ also produced low IPCE values and overall cell efficiencies were < 0.4%. These findings have been attributed to inefficient electron injection from a low-lying π* orbital on the dcbiq ligand into the TiO_2 conduction band. However our computational work on the $[Cu(dcbiq)_2]$ complex, and that of others,[30] suggests that the energy levels should be adequate for electron injection, although to the best of our knowledge its practical application in DSSCs has not been reported.

As established previously in the literature[4, 5, 24, 31] the design of copper(I) complexes needs to be carefully planned to prevent geometry changes upon oxidation from copper (I) to (II). Copper(II) complexes tend to flatten to square planar where coordination of a solvent molecule can occur, involving a large structural rearrangement and ultimately reducing the efficiency of electron transfer processes.[16] This can be prevented by constraining the copper(I) metal centre within a rigid environment by employing bulky ligands such as dcbiq.

Experimental

Synthesis of the complex was carried out in a nitrogen atmosphere. Reagents were obtained from major suppliers and used without further purification. IR spectra were recorded on a Perkin-Elmer 1600 FT IR spectrometer, with absorption maxima (ν_{max}) recorded in wavenumbers (cm^{-1}) and described as strong (s), medium (m), weak (w) and broad (br). Electronic absorption spectra were recorded on a Varian-Cary 50 Probe UV-Visible Spectrophotometer. NMR spectra were run on Brüker Avance 300, 400 or 500 MHz instruments at 298 K. Mass spectra were recorded with a micrOTOF electrospray time-of-flight (ESI-TOF) mass spectrometer (Brüker Daltonik). Elemental analysis was carried out by Stephen Boyer at London Metropolitan University. TiO_2 film thicknesses were measured using a NanoCalc-XR Thin Film Measurement System. Emission spectra were recorded at room temperature and at 77 K with 0.1 mM solutions of the dye in degassed ethanol or DCM, using a Fluoromax 2 fluorometer controlled by the ISAMain software

Photovoltaic measurements were carried out on a solar simulator (TS Space Systems), which used a 450 W xenon lamp as the light source and a potentiostat for recording the *I-V* data. The system had been calibrated with a standard silicon solar cell (type RS-OD-1) and an AM 1.5 filter was used. All cyclic voltammetry (CV) experiments were performed on a three electrode system with a μAutolab type II potentiostat and data were collected using either the Nova 1.5 or GPES software. For surface studies, the working electrode was a dyed TiO_2 film on fluorine-doped tin oxide (FTO) glass (dyed area 1 cm x 1.5 cm). For solution studies a boron doped diamond working electrode was used. A platinum counter electrode and an Ag/AgCl (3M KCl) reference electrode completed the cell. The CV experiments employed 0.1 M tetrabutylammonium hexafluorophosphate in MeCN as the electrolyte. In order to compare to potentials quoted in the literature, potentials in the results and discussion sections have been quoted versus the standard hydrogen electrode (SHE); where Ag/AgCl(3M) is +0.21V, SCE is +0.2412 and Fc/Fc^+ is +0.4. Details of electrode and cell preparation are given in the ESI.

All crystallographic data were collected on a Nonius kappa CCD diffractometer with MoKα radiation, λ = 0.71073 Å. T = 150(2) K throughout and all structures were solved by direct methods and refined on F^2 data using the SHELXL-97 suite of programs. Hydrogen atoms were included in idealised positions and refined using the riding model, except H3 and H2, which were freely refined and fully occupied. The R_{int} was higher than desirable, but the structure has been unambiguously determined. Despite copious efforts the crystals were small and poorly diffracting, hence the data was truncated to 2θ = 50º. The crystals contained significant amounts of diffuse solvent molecules (water and methanol). These were modelled as best as the data allowed. O(9A) and O(11) were half occupied water molecules the hydrogen atoms associated with these have been omitted from the model, both have been left anisotropic. Two half occupied molecules of methanol were also present in the asymmetric unit.

Synthesis of [Cu(2,2'-biquinoline-4,4'-dicarboxylic acid)][$HNEt_3$]

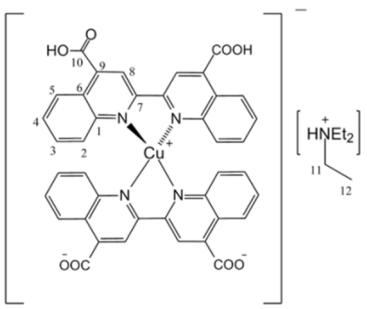

A solution of tetrakis(acetonitrile)copper(I) hexafluorophosphate (0.271 g, 0.73 mmol, 1.00 equiv) in MeCN (10 mL) was added via cannula to a stirring solution of 2,2'-biquinoline-4,4'-dicarboxylic acid (0.500 g, 1.46 mmol, 2.00 equiv) in DCM (10

mL). Triethylamine (0.40 mL, 2.92 mmol, 4.00 equiv) was added via syringe and the white slurry immediately became a clear, deep purple solution. The reaction was stirred for 16 h at rt. The solvent was removed under vacuum and the isolated purple solid purified by recrystallisation from MeOH and Et_2O. A dark purple powder was isolated by filtration and dried under vacuum to yield the desired product (0.217 g, 0.255 mmol, 35%). ^{1}H NMR (400 MHz, CD_3OD) δ_H/ppm 9.12 (s, 4H, H^8), 8.64 (d, J = 8.5 Hz, 4H, H^2), 7.80 (d, J = 8.5 Hz, 4H, H^5), 7.57 (t, J = 7.5 Hz, 4H, H^3), 7.38 (t, J = 7.5 Hz, 4H, H^4), 3.22 (q, J = 7.0, 12H, H^{11}), 1.31 (t, J = 7.0 Hz, 18H, H^{12}). ^{13}C NMR (125 MHz, CD_3OD) δ_C/ppm 172.8 (C^{10}), 153.6 (C^7), 149.4 (C^6), 147.6 (C^1), 132.4 (C^4), 130.0 (C^3), 129.0 (C^5), 128.1 (C^2), 128.0 (C^9), 119.0 (C^8), 47.9 (C^{11}), 9.2 (C^{12}). ESI-TOF MS *m/z* calcd for $[C_{40}H_{22}CuN_4O_8]^-$, 749.0739; found, 749.0750. ν_{max} (cm^{-1}) 2980 (m), 1712 (b), 1583 (m), 1560 (m). UV/VIS (MeOH) λ_{max} / nm (ε / dm^3 mol^{-1} cm^{-1}) 359 (55800), 564 (11700). Anal. calcd for $[C_{46}H_{38}CuN_5O_8].[PF_6C_6H_{16}N]$ (complex with co-crystallised $[PF_6][NEt_3]$): C, 56.80; H, 4.95; N, 7.64. Found: C, 57.08; H, 4.74; N, 7.30. $C_{188}H_{168}Cu_4N_{20}O_{40}$, M = 3601.58, purple, block, 0.1 × 0.1 × 0.2 mm^3, space group $C2/c$, V = 9057.5(6) Å^3, Z = 2, D_c = 1.322 g/cm^3, F_{000} = 3752, $2\theta_{max}$ = 50.1º, 48089 reflections collected, 7882 unique (R_{int} = 0.1592). Final *GooF* = 1.072, R_1 = 0.0700, wR_2 = 0.1692, R indices based on 5607 reflections with $I > 2\sigma$ (refinement on F^2), 627 parameters, 1 restraint, μ = 0.545 mm^{-1}.

Computational Details

All computations have been performed with the Gaussian 09 code[32], at the hybrid DFT level. More precisely, the M06 approach[33] was used in conjunction with a LANL2DZ basis set. Stationary points were characterized by harmonic frequency computations at the same theoretical level. Structures were also optimized including continuum solvation effects using the SMD solvent model, choosing methanol as solvent.[34]

To compute the UV-Vis transition of the title $[Cu(dcbiq)_2][HNEt_3]$ compound, the time-dependent (TD) DFT approach has been used at the same level. Only singlet-singlet transitions, i.e., spin-allowed transitions, with non-negligible oscillator strengths (f > 0.02) are reported and discussed. Computations were carried out to cover a spectral region down to 350 nm.

Results and Discussion

Synthesis and characterisation

The complex was synthesised under N_2 from the commercially available 2,2'-biquinoline-4,4'-dicarboxylic acid (dcbiq) and $[Cu(MeCN)_4][PF_6]$. Solubility of the ligand was poor; therefore, four equivalents of NEt_3 were added to the reaction mixture, resulting in the formation of a clear, deep purple solution. The dark purple solid obtained following recrystallisation from MeOH and Et_2O was identified as the desired complex. Full structural assignment was made using 2D ^{1}H and ^{13}C NMR. Crystals of suitable quality for X-ray diffraction were grown by slow evaporation from a MeOH solution of the dye. The crystal structure (Fig. 1) implies that in its solid-state form the complex exists with one biquinoline ligand being fully deprotonated and the other fully protonated (from analysis of C-O. C=O distances), resulting in a copper(I) 2,2'-biquinoline-4,4'-dicarboxylic acid anion, which is charge balanced with a $[HNEt_3]^+$ counterion. Negative mode ESI-MS showed a peak at *m/z* 749.075, corresponding to the molecular anion, $[M]^-$. There was no evidence of the $[PF_6]^-$ ion in the unit cell however its presence was noted through ^{31}P and ^{19}F NMR and also elemental analysis. Given the ratios of the triethylamine protons to those on the copper(I) complex, it was concluded that whilst one equivalent of triethylamine was charge balancing the copper(I) 2,2'-biquinoline-4,4'-dicarboxylic acid anion, a second equivalent was co-crystallising with the $[PF_6]^-$ anion. The crystal structure of the copper(I) complex indicates that the ligands are close to being orthogonal, in a pseudo tetrahedral geometry. Key bond lengths and angles (Fig. 1) are within the range of similar Cu(I) complexes reported in the literature.[7-9]

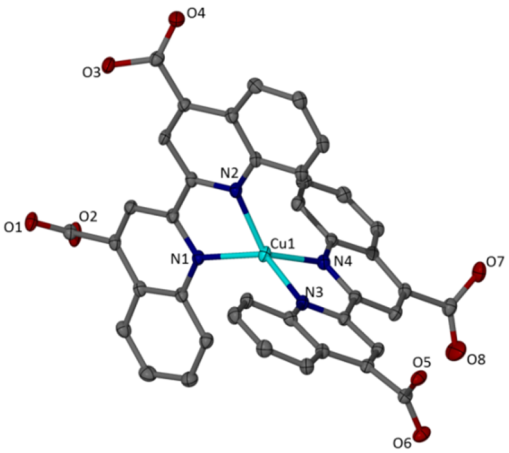

Fig. 1 Crystal structure of the $[Cu(2,2'\text{-biquinoline-4,4'-dicarboxylic acid})_2]^-$ anion. Selected bond lengths (Å): Cu(1)-N(1) = 2.015(4), Cu(1)-N(2) = 2.003(4), Cu(1)-(N3) = 2.002(4), Cu(1)-N(4) = 2.022(4) and angles (°): N(1)-Cu(1)-N(2) = 81.10(15), N(1)-Cu-N(3) = 132.33(16), N(1)-Cu-N(4) = 115.23(15). All hydrogen atoms have been removed for clarity, as have solvent of crystallisation and the $H[NEt_3]$ counterion.

UV/Vis absorption, surface coverage of dye and emission

The electronic absorption spectrum for $[Cu(dcbiq)_2][HNEt_3]$ in methanol (inset Fig. 2(a)) shows that the extended conjugation of the 2,2'-biquinoline ligand induces a so-called "red shift" in the peak absorbance of the dye compared to its 2,2'-bipyridine analogues. The peak absorptions at 345nm and 357nm are attributed to ligand based $\pi \rightarrow \pi^*$ transitions and at 564 nm to a metal-to-ligand charge transfer (MLCT) transition. These allocations are supported by computational data, which are discussed below. The molar extinction coefficient for $\lambda_{(max)}$ 564 nm is 11,700 $M^{-1}cm^{-1}$ in MeOH, which is comparable to the reported values for the less conjugated bipyridine analogue[7] [Cu(6,6'-dimethyl-2,2'-bipy-4,4'-dicarboxylic acid)][Cl], of 9900 $M^{-1}cm^{-1}$ at 483 nm and the benchmark ruthenium(II) complex[35] N3, which has a molar extinction coefficient of 14,200 $M^{-1}cm^{-1}$ at 534 nm.

UV/Vis spectra of the dye anchored to the TiO_2 surface were also recorded for films dyed for increasing periods of time (Fig.

2(a)) and the adsorption isotherms show typical behaviour for dye uptake on a TiO_2 film.[36-39] The $\lambda_{(max)}$ value for the surface bound dye shifts to a slightly higher energy in comparison to that measured in solution (552 nm compared to 564 nm). The same behaviour is observed for the heteroleptic complex[13] and is attributed to the variation in protonation between the dcbiq ligand on the surface (fully deprotonated) and in solution. The shift may also be due to aggregation effects of the dye on the surface.[40] To calculate the amount of dye adsorbed on the TiO_2 films, the dye was then desorbed by immersion in 1 M KOH (aq) for 45 minutes. The dye complex decomposed under the basic conditions used for desorption, resulting in colourless KOH (aq) solutions, therefore the dye coverage was calculated from the amount of dcbiq ligand in solution, using the absorbance at 332nm, (ε = 26,100 dm^3 mol^{-1} cm^{-1}). The calibration measurements were made using dye solutions in 1 M KOH, which were also colourless. After overnight dyeing, the the surface coverage is $\approx 10 \times 10^{-8}$ mol $cm^{-2}$of geometric film area. This figure is comparable to reported data for the analogous ruthenium biquinoline complex[29] and the typical ruthenium dyes N3[35] and N719.[35, 36, 41] In our measurements TiO_2 film thicknesses were typically between 9 and 10 microns, measured by reflectometry. Dye coverage was also estimated from the UV/Vis measurements of the dyed TiO_2 films and very similar results were seen.

Emission spectroscopy studies on a degassed 0.1 mM ethanol solution of $[Cu(dcbiq)_2][HNEt_3]$ produced a broad emission peak at 400nm following excitation at 330 nm, attributed to fluorescence from the ligand-based π^* excited state. When cooled to 77 K, three peaks at 500, 536 and 584 nm were observed following the 330 nm excitation, interpreted as phosphorescence from the same state. Emission from the MLCT excited state was not observed at either temperature or over the large range of excitation wavelengths tried. When the solvent was changed to DCM (degassed), fluorescence was observed at room temperature following excitation at 490 and at 520 nm (Fig. 3). It is difficult to determine whether this is emission from a ligand-based π^* state or the MLCT state, as the excitation wavelength is midway between that expected for either state, with respect to the electronic absorption spectrum (which was also carried out in DCM for direct comparison).

Difficulties in obtaining adequate luminescence data for heteroleptic copper complexeswere reported by Odobel *et al*, who reasoned that the lack of emission was either due to a quenching mechanism from a flattening of the complex, or else a non-radiative decay process.[13] Such explanations may similarly be applicable in the case of the homoleptic species.

(a)(

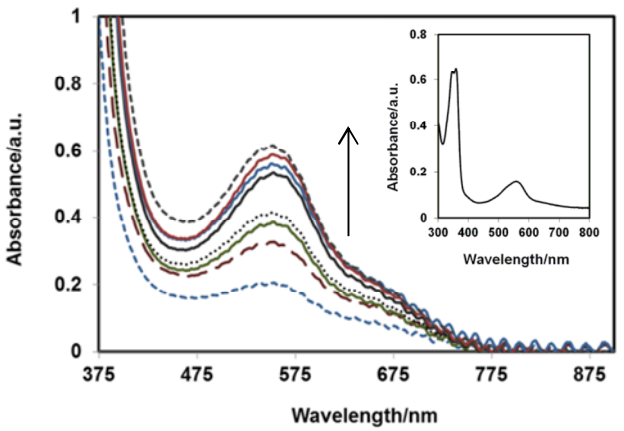

b)

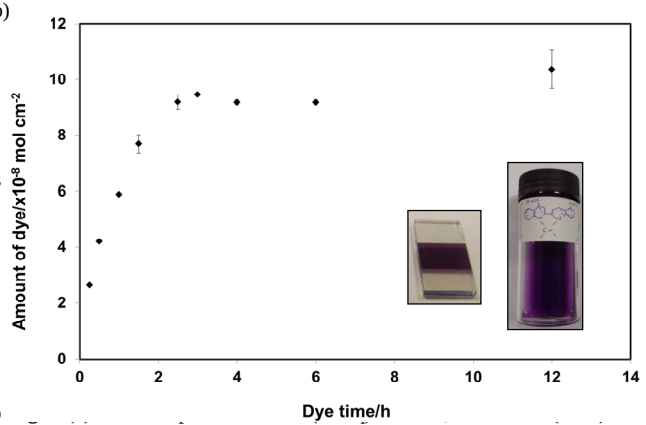

UV/Vis spectra of the dye adsorbed on TiO_2 films at increasing dye times; 15 min (---), 30 min (− − −), 1h ( ), 2h (·····), 3h ( ), 4h ( ), 6h ( ), 12h (---). (b) Amount of $[Cu(dcbiq)_2]$ $[HNEt_3]$ adsorbed on the TiO_2 films with increasing dye time (n=2, error bars show one standard deviation), measured by UV/Vis, following dye desorption from the films into 1M KOH and (inset) a sample solution and a dyed film.

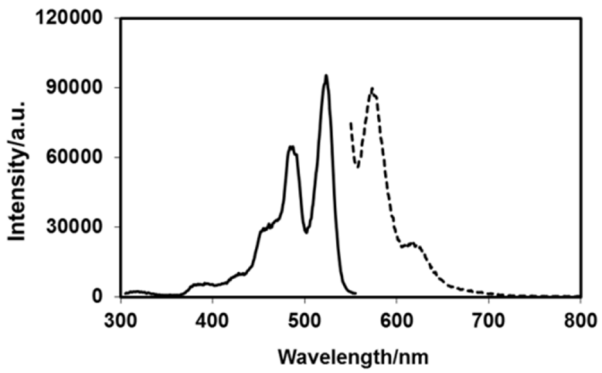

Fig. 3 Emission spectrum of $[Cu(dcbiq)_2][HNEt_3]$ in DCM at room temperature following excitation at 520 nm (----) and the excitation acquisition (—) for emission at 575 nm.

Computational Analysis

Solvent effects have to be taken into account to correctly describe the orbital splitting in the case of the deprotonated form of the bare 2,2'-biquinoline-4,4'-dicarboxylic acid ligand.[42] The computations indicate that the most stable structure of the copper(I) 2,2'-biquinoline-4,4'-dicarboxylic acid anion is in

excellent agreement with the experimental findings (See Supplementary Material). The computed structure shows a slight deviation from C_2 symmetry, with the protons located on different ligands. There was a slight discrepancy here with the experimental crystallographic data, which found the protons to be located on the same ligand. However, the structures are energetically very similar (the energy difference including the zero-point energy correction, is only 1.1 kcal/mol), thus the locations of the protons in the solid state may be influenced by forces such as intermolecular hydrogen bonding.

A detailed analysis of the highest occupied and the lowest unoccupied molecular orbitals of the title complex is summarized in Table 1. The largest contributions for the HOMO, HOMO-1, and HOMO-2 are the antibonding combinations (Fig. 4) of the nitrogen lone pairs with an important percentage of the t_2 metal orbitals (ranging from 22% to 63%). At lower energy (~1 eV with respect to the HOMO), there are also other orbitals with a predominant Cu-d character (35%, 43%, respectively).

Table 1. Energies and Composition of the Higher Occupied and Lower Unoccupied Molecular Orbitals of the [Cu(2,2'-biquinoline-4,4'-dicarboxylic acid)$_2$]$^-$ anion.

MO	occ	E(eV)	Cu (% contribution)
LUMO+5	0	-1.23	
LUMO+4	0	-1.24	
LUMO+3	0	-1.86	
LUMO+2	0	-1.89	
LUMO+1	0	-2.73	
LUMO	0	-2.81	
HOMO	2	-5.78	58 (d_{xy})
HOMO-1	2	-6.11	63 (d_{xz})
HOMO-2	2	-6.68	22 (d_{yz})
HOMO-3	2	-6.76	35 (d_{z2}, d_{x2-y2})
HOMO-4	2	-6.86	43 (d_{yz})
HOMO-5	2	-7.02	
HOMO-6	2	-7.03	

The LUMOs are antibonding orbitals which arise from the carbon and the nitrogen p orbitals and have a significant contribution from the carboxylic acid groups. Like their Ru(II) congeners, in a dye sensitized solar cell the carboxylic acid groups act as anchoring groups to the TiO_2 semiconductor surface, favouring the electron injection process from the dye excited state into the semiconductor conduction band.[43] Note that the computed HOMO energy (-5.78 eV) is in excellent agreement with the experimental value obtained from electrochemical analysis. The estimated HOMO-LUMO gap is 2.97 eV.

The excitation energies and oscillator strengths for the first two absorption bands are reported in Table 2, together with the composition of the solution vectors in terms of the most relevant transitions. In the energy range investigated, two bands clearly appear. The first band, with a maximum absorption located at 563 nm, which is in excellent agreement with the experimental value (564 nm), involves multiple MLCT transitions, mainly excitations from the HOMO and HOMO-1, corresponding to one-electron excitations from t_2-π^*/t_2-π to π^*-ligand levels. The second absorption band, with a maximum at about 360 nm, involves transitions mainly from HOMO-5 and HOMO-9 to the lowest unoccupied π^* orbitals localized on the ligand.

Fig. 4 LUMO and the five highest occupied molecular orbitals of the [Cu(2,2'-biquinoline-4,4'-dicarboxylic acid)$_2$]$^-$ anion (Isodensity contour = 0.04).

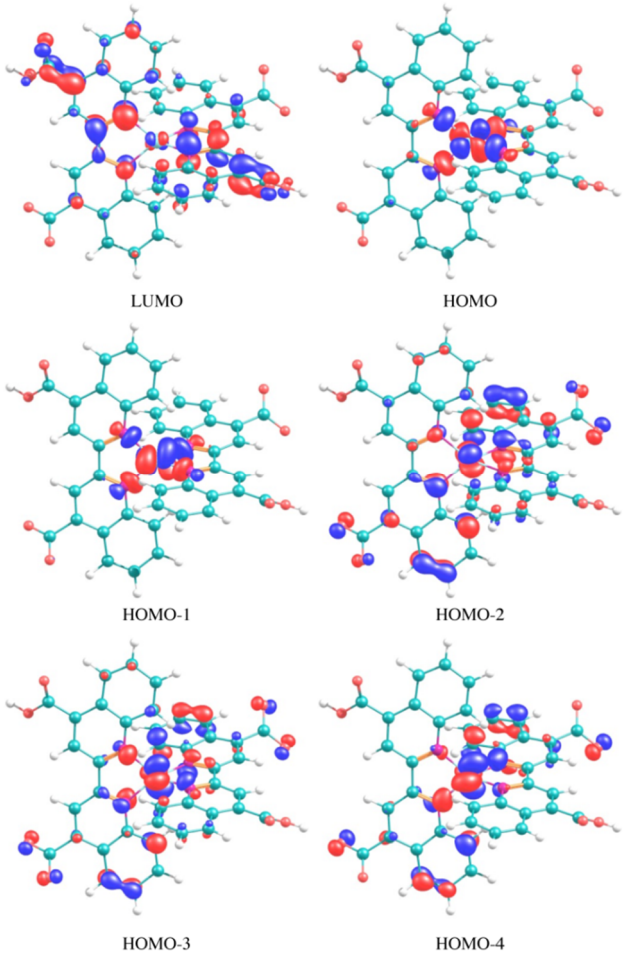

Table 2. Wavelength, oscillator strength and composition of the most important optical transitions.

λ (nm)	f	Composition
692	0.036	HOMO-1 → LUMO+1 (18%)
		HOMO → LUMO (79%)
563	0.163	HOMO-1 → LUMO+1 (79%)
419	0.041	HOMO → LUMO+2 (81%)
375	0.038	HOMO-4 → LUMO (41%)
368	0.023	HOMO-4 → LUMO+1 (45%)
		HOMO-5 → LUMO +1 (10%)
361	0.114	HOMO-5 → LUMO (40%)
		HOMO-9 → LUMO (29%)
359	0.057	HOMO-8 → LUMO (11%)
		HOMO-6 → LUMO (44%)
355	0.082	HOMO-12 → LUMO (46%)
350	0.039	HOMO-8 → LUMO+1 (19%)
		HOMO-7 → LUMO (40%)

Electrochemistry

Cyclic voltammograms (CVs) were measured for $[Cu(dcbiq)_2][HNEt_3]$ both in solution and on a TiO_2 surface. Electrochemistry of the dye in solution was carried out using a boron doped diamond working electrode with a background electrolyte of 0.1 M $[Bu_4N][PF_6]$ in acetonitrile. CVs were recorded over a range of scan rates and dye concentrations following the addition of aliquots of a methanolic solution of the dye (Fig. 5). At slower scan rates oxidation and reduction peaks were observed, which were assigned to the Cu(I)/(II) couple, although the peak separation was large (≈ 650 mV). At faster scan rates (≥ 5 V/s) the electrochemistry was less reversible and the reduction peak almost entirely disappeared.

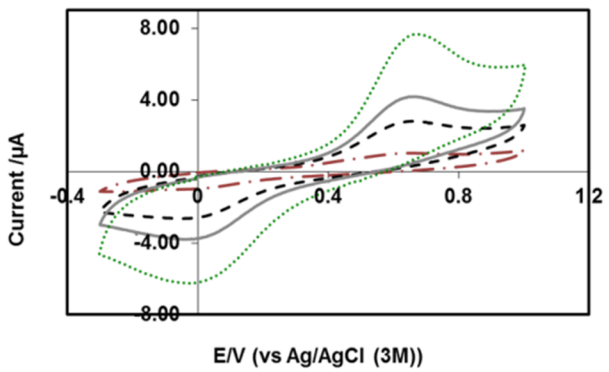

Fig. 5 CVs at increasing scan rates of $[Cu(dcbiq)_2][HNEt_3]$ in solution; 0.1 V/s (- - -), 0.5 V/s (- - -), 1 V/s (—), 3 V/s (·····). (vs Ag/AgCl, 0.1 M $[Bu_4N][PF_6]$ in MeCN electrolyte)

CVs were also measured for dye adsorbed onto nanoporous TiO_2 films doctor bladed onto FTO glass (Fig. 6). The films were dyed overnight in a 0.3 mM MeOH solution of $[Cu(dcbiq)_2][HNEt_3]$. As the TiO_2 is an insulator under the conditions used in the CV, electron transfer to and from absorbed dye molecules occurs via dye molecules in contact with bare FTO at the base of the pores. Observation of dye electrochemistry therefore indicates dye coverage throughout the porous TiO_2 network to the FTO contact.

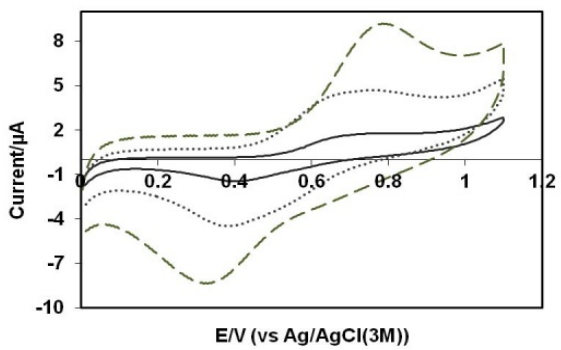

Fig. 6 CVs at increasing scan rates of $[Cu(dcbiq)_2][HNEt_3]$ adsorbed on a TiO_2 film; 0.01 V/s (—), 0.05 V/s (·····), 0.1 V/s (– – –) (vs Ag/AgCl, 0.1 M $[Bu_4N][PF_6]$ in MeCN electrolyte)

CVs of surface adsorbed dye showed a peak separation of ≈ 300 mV at 10 mVs^{-1}, although the separation increased with scan rate. The difference in peak separation between the solution and surface experiments suggests that the reorganisation energy is larger in solution than on the surface.

The copper(I) complex appears to be almost tetrahedral in the crystal structure (d^{10}), however it is expected that following oxidation the copper(II) species will be closer to square planar (d^9). The electrochemistry suggests that the complex switches geometry more easily in solution, meaning the reduction step during the reverse scan has to overcome a large reorganisation energy to enable the dye to return to its tetrahedral state. The dye is more constrained on the surface of the TiO_2 film in its tetrahedral arrangement; therefore, a geometry change is less viable. With a peak separation of ≈ 300 mV, the electron transfer kinetics are too slow for the cycle to be ideally reversible, therefore the electrochemical behaviour is best described as quasi-reversible. The series resistance for the surface bound experiments was measured to be 138 Ω by impedance spectroscopy. This value is a sum of the resistance of the solution, the FTO electrode and the contacts. The FTO electrodes were ~2.25 cm long and had a resistance of 13 Ω□; therefore they will make a large contribution to the series resistance. It should be noted that compensating for the series resistance using the IR compensation function changed the shape of the voltammograms slightly but did not reduce the peak separation.

The peak oxidation potential, E_p^{ox}, was +0.78 V and the peak reduction potential, E_p^{red}, was +0.33 V. Vatsadze *et al.* reported the electrochemistry of the similar complex $[CuL_2][Cl]$ where L = di-*n*-hexyl 2,2´-biquinoline-4,4´-dicarboxylate.[44] The Cu(I) to (II) oxidation occurred at E_p^{ox} = +0.74 V versus Ag/AgCl (sat. KCl), which is in good agreement with our findings. For the same complex, but with a $[BF_4]^-$ counterion, the group reported E_p^{ox} = +0.75 V and E_p^{red} = +0.36 V (vs Ag/AgCl/KCl)[45] which also implies that the counterion has little effect on energy levels in the dye.

The half wave potential, $E_{1/2}$, for $[Cu(dcbiq)_2][HNEt_3]$ is +0.56 V versus Ag/AgCl (or +0.77 V versus the normal hydrogen electrode, SHE), which is more than adequate for dye regeneration given that the standard potential of the I^-/I_3^- redox couple is +0.35 V (vs SHE).[46] This was confirmed by probing the reduction of the dye's excited state by iodide using cyclic voltammetry. A dyed TiO_2 film was used as the working electrode and an increasing concentration of LiI was added (from 0 M to 3.39 mM in a solution of 0.1 M $[Bu^n_4N][PF_6]$ in MeCN). An EC' mechanism was observed (Fig. 7), where E refers to an electrode step and C' is a catalytic chemical process.

E: $D - e^- \longrightarrow D^+$

C': $D^+ + 3/2\ I^- \longrightarrow D + 1/2\ I_3$

A large increase in the oxidative current was observed with increasing concentration of iodide since, as the dye's ground state is regenerated in the catalytic step, it is rapidly re-oxidised at the anode. The reduction peak initially decreases then disappears completely as the iodide rapidly reoxidises the reduced species.

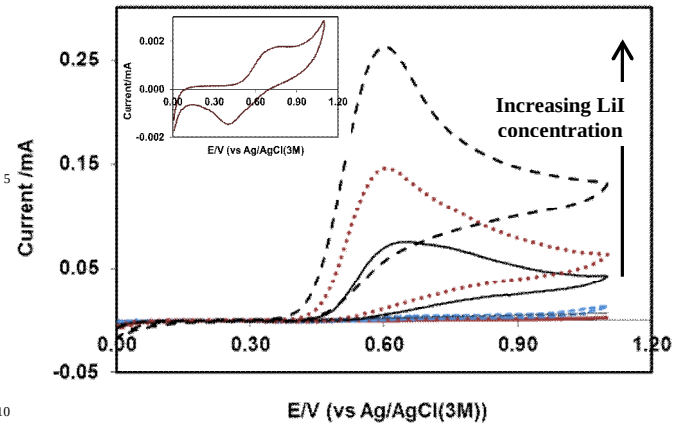

Fig. 7 CV of a [Cu(dcbiq)2][HNEt3] dyed film at a scan rate of 0.01 V/s with increasing concentrations of LiI; 3.39 mM (- - -), 2.78 mM (···), 1.55 mM (——), 0.31 mM (- - -), 0 mM (——). The inset shows a zoomed in view of the CV with 0 mM LiI (Vs Ag/AgCl, 0.1 M $[Bu_4N][PF_6]$ in MeCN electrolyte).

The half wave potential is closely related to the HOMO level of the dye, given that the onset of the oxidative wave indicates that electrons are starting to be removed from the ground state. Using the CV data we estimate the position of the HOMO for the complex to be -5.27 eV.[47] The excited state potential can be estimated by adding the zero-zero transition energy ($E^{0\text{-}0}$), obtained from emission spectroscopy, to $E_{1/2}$. So with an $E^{0\text{-}0}$ value of 2.426 eV the resulting first excited state energy is -2.844 eV, which would be sufficient for injection into the TiO_2 conduction band. Given the ambiguity in the emission data we are cautious in this conclusion, however this value is in excellent agreement with the computationally derived LUMO energy (-2.81 eV). Unfortunately, the IPCE spectrum showed an external quantum efficiency of no greater than 1% between the key wavelengths of 450 to 650 nm, indicating that electron injection is not occurring from the LUMO or the first excited state energy level. We conclude that there are likely lower energy, non-emissive states into which the electrons are being promoted, or else rapidly decaying to, but not successfully injected from.

DSSC performance

The performance of $[Cu(dcbiq)_2][HNEt_3]$ in a DSSC was studied. Cells were prepared following overnight dyeing of the TiO_2 films from a 0.3 mM methanol solution. Overall efficiencies were poor compared to those reported for other copper(I) dyes and generally < 0.1 %. As mentioned previously, we concluded that the problem was most likely inefficient electron injection into the TiO_2 conduction band, through either mismatched excited state energy levels or due to an excited state lifetime that was too short. Efforts to overcome any energy level mismatch were made by trying to optimise the cell environment to be more compatible with the dye. Cells were constructed using a reduced concentration of, or omitting entirely, the 4-*tert*-butylpyridine (4-TBP). It is known that 4-TBP in the electrolyte increases the V_{oc} due to both a shift of the TiO_2 conduction band edge to a more negative potential and through reducing the recombination of electrons in the TiO_2 with I_3^- in the electrolyte.[48] Therefore by removing the 4-TBP we aimed to achieve the opposite effect and improve electron injection into the TiO_2 conduction band. Although there was no overall improvement in cell efficiency in this way, the V_{oc} decreased and the I_{sc} increased slightly (Fig. 8).

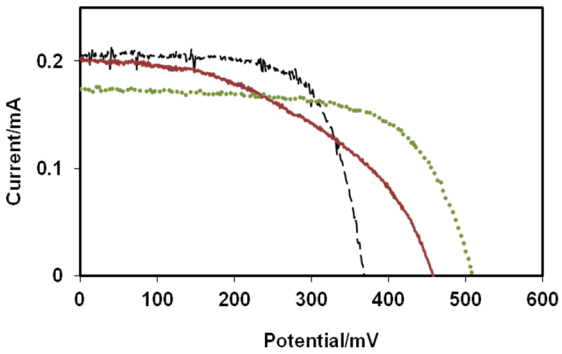

Fig. 8 *I-V* curves for DSSCs prepared with $[Cu(dcbiq)_2][HNEt_3]$ and varying concentrations of 4-TBP in the electrolyte; 0.5 M (·····), 0.3 M (——) and 0 M (- - -).

The fully-protonated free acid and the sodium salt of the copper(I) biquinoline complex were also synthesized for comparison to the $[HNEt_3]^+$ complex (Table 3). Cell efficiencies were slightly improved, most notably with the sodium salt through the improvement of the cell V_{oc}. This increased V_{oc} indicates a negative shift of the conduction band potential, which is expected for the fully deprotonated form of the complex.[49] Comparison of photovoltage between the three species also affirms that the extent of surface protonation in the cell when $[NEt_3]$ used is midway between that of the free acid and the fully deprotonated sodium salt, as evidenced through the crystal structure.

Table 3. cell characteristics for 1cm² DSSCs prepared with variants of the copper(I) biquinoline complex

Cell (Dye)	J_{sc} / mA	V_{oc} / mV	FF	η / %
1 ($-COO^-$)(Na^+)	0.204	629	0.69	0.089
2 ($-COO^-$)(Na^+)	0.224	623	0.72	0.100
3 ($-COO^-$)(Na^+)	0.226	600	0.70	0.095
4 (-COOH)	0.206	515	0.71	0.075
5 (-COOH)	0.235	511	0.66	0.080
6 (-COOH)	0.233	499	0.66	0.077
7 ($-COO^-$)($HNEt_3$)$^+$	0.197	523	0.66	0.068
8 ($-COO^-$)($HNEt_3$)$^+$	0.199	528	0.69	0.073

Conclusions

A [Cu(2,2'-biquinoline-4,4'-dicarboxylic acid)] complex has been synthesised and extensively studied with respect to application in a dye-sensitized solar cell. To the best of our knowledge this is the first report of this complex being trialled in a DSSC. The dye has a good extinction coefficient and electrochemical studies show that the ground state can be regenerated by iodide. In addition the dye gave good surface coverage and was stable to electrochemical cycling even at slow scan rates (10 mVs^{-1}), in contrast many ruthenium dyes degrade at this scan rate.

Computer modelling suggested that the key dye excited state should be high enough in energy to inject electrons in the TiO_2 conduction band. Despite this cell efficiencies were very low. Modification of the ligand may allow improved performance in DSSC.

Acknowledgements

We thank the EPSRC for funding (DTC studentship for Kathryn Wills, Grant EP/G03768X/1) and Dr Neil Robertson and Tracy Hewat at the University of Edinburgh for their help with the emission spectroscopy work. We thank Dr. G. Kociok-Köhn for assistance with X-ray structure refinement.

Notes and references

1. B. O' Regan and M. Grätzel, *Nature*, 1991, **353**, 737-740.
2. J. Desilvestro, M. Gratzel, L. Kavan, J. Moser and J. Augustynski, *J. Am. Chem. Soc.*, 1985, **107**, 2988-2990.
3. M. K. Nazeeruddin, E. Baranoff and M. Grätzel, *Sol. Energy*, 2011, **85**, 1172-1178.
4. N. Robertson, *ChemSusChem*, 2008, **1**, 977-979.
5. A. H. Rendondo, E. C. Constable and C. E. Housecroft, *Chimia*, 2009, **63**, 205-207.
6. T. Bessho, E. C. Constable, M. Grätzel, A. H. Redondo, C. E. Housecroft, W. Kylberg, M. K. Nazeeruddin, M. Neuburger and S. Schaffner, *Chem. Commun.*, 2008, 3717-3719.
7. E. C. Constable, A. H. Redondo, C. E. Housecroft, M. Neuburger and S. Schaffner, *Dalton Trans.*, 2009, 6634-6644.
8. B. Bozic-Weber, V. Chaurin, E. C. Constable, C. E. Housecroft, M. Meuwly, M. Neuburger, J. A. Rudd, E. Schoenhofer and L. Siegfried, *Dalton Trans.*, 2012, **41**, 14157-14169.
9. B. Bozic-Weber, E. C. Constable, C. E. Housecroft, P. Kopecky, M. Neuburger and J. A. Zampese, *Dalton Trans.*, 2011, **40**, 12584-12594.
10. C. L. Linfoot, P. Richardson, T. E. Hewat, O. Moudam, M. M. Forde, A. Collins, F. White and N. Robertson, *Dalton Trans.*, 2010, **39**, 8945-8956.
11. X. Q. Lu, S. X. Wei, C. M. L. Wu, S. R. Li and W. Y. Guo, *J. Phys. Chem. C*, 2011, **115**, 3753-3761.
12. B. Bozic-Weber, E. C. Constable, C. E. Housecroft, M. Neuburger and J. R. Price, *Dalton Trans.*, 2010, **39**, 3585-3594.
13. M. Sandroni, M. Kayanuma, A. Planchat, N. Szuwarski, E. Blart, Y. Pellegrin, C. Daniel, M. Boujtita and F. Odobel, *Dalton Trans.*, 2013, **42**, 10818-10827.
14. B. Bozic-Weber, E. C. Constable, S. O. Furer, C. E. Housecroft, L. J. Troxler and J. A. Zampese, *Chem. Commun.*, 2013.
15. L. N. Ashbrook and C. M. Elliott, *J. Phys. Chem. C*, 2013, **117**, 3853-3864.
16. J. Huang, O. Buyukcakir, M. W. Mara, A. Coskun, N. M. Dimitrijevic, G. Barin, O. Kokhan, A. B. Stickrath, R. Ruppert, D. M. Tiede, J. F. Stoddart, J.-P. Sauvage and L. X. Chen, *Angew. Chem.-Int. Edit.*, 2012, **51**, 12711-12715.
17. B. Bozic-Weber, S. Y. Brauchli, E. C. Constable, S. O. Fuerer, C. E. Housecroft and I. A. Wright, *Phys. Chem. Chem. Phys.*, 2013, **15**, 4500-4504.
18. Y. Chen, Z. Zeng, C. Li, W. Wang, X. Wang and B. Zhang, *New Journal of Chemistry*, 2005, **29**, 773-776.
19. B. E. Hardin, H. J. Snaith and M. D. McGehee, *Nature Photonics*, 2012, **6**, 162-169.
20. B. C. O'Regan, I. López-Duarte, M. V. Martínez-Díaz, A. Forneli, J. Albero, A. Morandeira, E. Palomares, T. Torres and J. R. Durrant, *J. Am. Chem. Soc.*, 2008, **130**, 2906-2907.
21. A. Mishra, M. K. R. Fischer and P. Bäuerle, *Angewandte Chemie International Edition*, 2009, **48**, 2474-2499.
22. H. N. Tsao , C. Yi , T. Moehl, J.-H. Yum, S. M. Zakeeruddin, M. K. Nazeeruddin and M. Grätzel, *ChemSusChem*, 2011, **4**, 591-594.
23. A. Yella, H.-W. Lee, H. N. Tsao, C. Yi, A. K. Chandiran, M. K. Nazeeruddin, E. W.-G. Diau, C.-Y. Yeh, S. M. Zakeeruddin and M. Grätzel, *Science*, 2011, **334**, 629-634.
24. B. Gil and S. M. Draper, *Switching-on: The Copper Age, in Ideas in Chemistry and Molecular Sciences: Advances in Nanotechnology, Materials and Devices*, Wiley-VCH, 2010.
25. P. K. Smith, R. I. Krohn, G. T. Hermanson, A. K. Mallia, F. H. Gartner, M. D. Provenzano, E. K. Fujimoto, N. M. Goeke, B. J. Olson and D. C. Klenk, *Anal. Biochem.*, 1985, **150**, 76-85.
26. R. D. Braun, K. J. Wiechelman and A. A. Gallo, *Analytica Chimica Acta*, 1989, **221**, 223-238.
27. M. K. Nazeeruddin, E. Muller, R. Humphry-Baker, N. Vlachopoulos and M. Gratzel, *Journal of the Chemical Society-Dalton Transactions*, 1997, 4571-4578.
28. S. Ruile, O. Kohle, P. Pechy and M. Grätzel, *Inorganica Chimica Acta*, 1997, **261**, 129-140.
29. A. Islam, H. Sugihara, L. P. Singh, K. Hara, R. Katoh, Y. Nagawa, M. Yanagida, Y. Takahashi, S. Murata and H. Arakawa, *Inorganica Chimica Acta*, 2001, **322**, 7-16.
30. J. Baldenebro-Lopez, J. Castorena-Gonzalez, N. Flores-Holguin, J. Almaral-Sanchez and D. Glossman-Mitnik, *Int. J. Mol. Sci.*, 2012, **13**, 16005-16019.
31. R. M. Williams, L. De Cola, F. Hartl, J. J. Lagref, J. M. Planeix, A. De Cian and M. W. Hosseini, *Coord. Chem. Rev.*, 2002, **230**, 253-261.
32. M. J. Frisch, G. W. Trucks, H. B. Schlegel, G. E. Scuseria, M. A. Robb, J. R. Cheeseman, G. Scalmani, V. Barone, B. Mennucci, G. A. Petersson, H. Nakatsuji, M. Caricato, X. Li, H. P. Hratchian, A. F. Izmaylov, J. Bloino, G. Zheng, J. L. Sonnenberg, M. Hada, M. Ehara, K. Toyota, R. Fukuda, J. Hasegawa, M. Ishida, T. Nakajima, Y. Honda, O. Kitao, H. Nakai, T. Vreven, J. A. Montgomery, J. E. Peralta, F. Ogliaro, M. Bearpark, J. J. Heyd, E. Brothers, K. N. Kudin, V. N. Staroverov, R. Kobayashi, J. Normand, K. Raghavachari, A. Rendell, J. C. Burant, S. S. Iyengar, J. Tomasi, M. Cossi, N. Rega, J. M. Millam, M. Klene, J. E. Knox, J. B. Cross, V. Bakken, C. Adamo, J. Jaramillo, R. Gomperts, R. E. Stratmann, O. Yazyev, A. J. Austin, R. Cammi, C. Pomelli, J. W. Ochterski, R. L. Martin, K. Morokuma, V. G. Zakrzewski, G. A. Voth, P. Salvador, J. J. Dannenberg, S. Dapprich, A. D. Daniels, Farkas, J. B. Foresman, J. V. Ortiz, J. Cioslowski and D. J. Fox, Wallingford CT, 2009.
33. Y. Zhao and D. G. Truhlar, *Theoretical Chemistry Accounts*, 2008, **120**, 215-241.

34. A. V. Marenich, C. J. Cramer and D. G. Truhlar, *Journal of Physical Chemistry B*, 2009, **113**, 6378-6396.
35. M. K. Nazeeruddin, A. Kay, I. Rodicio, R. Humphry-Baker, E. Muller, P. Liska, N. Vlachopoulos and M. Grätzel, *J. Am. Chem. Soc.*, 1993, **115**, 6382-6390.
36. E. Dell'Orto, L. Raimondo, A. Sassella and A. Abbotto, *Journal of Materials Chemistry*, 2012, **22**, 11364-11369.
37. M. Durr, A. Schmid, M. Obermaier, A. Yasuda and G. Nelles, *Journal of Physical Chemistry A*, 2005, **109**, 3967-3970.
38. P. J. Holliman, B. V. Velasco, I. Butler, M. Wijdekop and D. A. Worsley, *Int J Photoenergy*, 2008.
39. A. Fillinger and B. A. Parkinson, *Journal of the Electrochemical Society*, 1999, **146**, 4559-4564.
40. S. Agrawal, M. Pastore, G. Marotta, M. A. Reddy, M. Chandrasekharam and F. De Angelis, *The Journal of Physical Chemistry C*, 2013.
41. A. Peic, D. Staff, T. Risbridger, B. Menges, L. M. Peter, A. B. Walker and P. J. Cameron, *J. Phys. Chem. C*, 2011, **115**, 613-619.
42. F. De Angelis, S. Fantacci and A. Selloni, *Chemical Physics Letters*, 2004, **389**, 204-208.
43. S. Fantacci, F. De Angelis and A. Selloni, *J. Am. Chem. Soc.*, 2003, **125**, 4381-4387.
44. S. Z. Vatsadze, A. V. Dolganov, A. V. Yakimanskii, M. Y. Goikhman, I. V. Podeshvo, K. A. Lyssenko, A. L. Maksimov and T. V. Magdesieva, *Russ. Chem. Bull.*, 2010, **59**, 724-732.
45. T. V. Magdesieva, A. V. Dolganov, P. M. Polestchuk, A. V. Yakimanskii, M. Y. Goikhman, I. V. Podeshvo and V. V. Kudryavtsev, *Russ. Chem. Bull.*, 2007, **56**, 1380-1389.
46. G. Boschloo and A. Hagfeldt, *Accounts Chem. Res.*, 2009, **42**, 1819-1826.
47. F. Brovelli, B. L. Rivas, J. C. Bernede, M. A. del Valle, F. R. Diaz and Y. Berredjem, *Polymer Bulletin*, 2007, **58**, 521-527.
48. G. Boschloo, L. Haggman and A. Hagfeldt, *Journal of Physical Chemistry B*, 2006, **110**, 13144-13150.
49. M. K. Nazeeruddin and M. Grätzel, *Comprehensive Coordination Chemistry II*, Elsevier, **2004** , Chap. 16, p. 719.